
Article:
Tellez-Gabriel, M., Charrier, C., Brounais-Le Royer, B. et al. (4 more authors) (2017) Analysis of gap junctional intercellular communications using a dielectrophoresis-based microchip. European Journal of Cell Biology, 96 (2). pp. 110-118. ISSN 0171-9335

https://doi.org/10.1016/j.ejcb.2017.01.003

Analysis of gap junctional intercellular communications using a dielectrophoresis-based microchip

Marta TELLEZ-GABRIEL[1,2,3], Céline CHARRIER[1,2], Bénédicte BROUNAIS-LE ROYER[1,2], Mathilde MULLARD [1,2], BROWN Hannah K.[4,5], Franck VERRECCHIA[1,2] and Dominique HEYMANN[1,2,4,5]

[1]INSERM, UMR 957, Equipe LIGUE Nationale Contre le Cancer 2012, Nantes 44035, France

[2]Université de Nantes, Nantes atlantique universités, Pathophysiology of Bone Resorption and Therapy of Primary Bone Tumours, Nantes, France

[3]Laboratotio Hematologia Oncologica y de Transplantes, Institut Investigacions Biomèdiques (IBB) Sant Pau, Hospital de la Santa Creui Sant Pau, 08025 Barcelona, Spain

[4]Department of Oncology and Metabolism, The University of Sheffield, Sheffield, UK

[5]European Associated Laboratory, INSERM, Sarcoma Research Unit, University of Sheffield, Medical School, S10 2RX, Sheffield, UK

Keywords: Gap junctional intercellular communication, Dielectrophoresis device, Bone microenvironment

*** Correspondance to:**

Prof. Dominique HEYMANN

Department of Oncology and Metabolism

The University of Sheffield

Medical School, Beech Hill Road

S10 2RX Sheffield, UK

Phone: +44 (0) 114 226 8464

E-mail: dominique.heymann@sheffield.ac.uk

ABSTRACT

Gap junctions are transmembrane structures that directly connect the cytoplasm of adjacent cells, making intercellular communications possible. It has been shown that the behaviour of several tumours – such as bone tumours – is related to gap junction intercellular communications (GJIC). Several methodologies are available for studying GJIC, based on measuring different parameters that are useful for multiple applications, such as the study of carcinogenesis for example. These methods nevertheless have several limitations. The present manuscript describes the setting up of a DEP-based lab-on-a-chip platform for the real-time study of Gap Junctional Intercellular Communication between osteosarcoma cells and the main cells accessible to their microenvironment. We conclude that using the DEParray technology for the GJIC assessment has several advantages comparing to current techniques. This methodology is less harmful for cells integrity; cells can be recovered after interaction to make further molecular analysis; it is possible to study GJIC in real time; we can promote cell interactions using up to five different populations. The setting up of this new methodology overcomes several difficulties to perform experiments for solving questions about GJIC process that we are not able to do with current technics.

INTRODUCTION

Gap Junctional Intercellular Communication (GJIC) consists of intercellular exchange of low molecular weight molecules, and is the only means for direct contact between cytoplasms of adjacent animal cells. Gap junctions are specialised plasma membrane structures consisting of transmembrane channels, themselves composed of proteins called connexins (Cx) that directly link the cytoplasm of adjacent cells, thereby enabling direct intercellular communication (Nielsen et al., 2012). The permeability of Gap junction channels is finely regulated at the transcriptional and post-translational level *via* cycles of connexin phosphorylation, intracellular Ca^{2+} or H^{+} concentrations, or by hormones (e.g. oestrogen, progesterone, androgens...)(Firestone and Kapadia, 2012, Zhang and Shaw, 2013). Many physiological roles have been proposed for GJIC such as an major involvement in cellular homeostasis and integrator of cellular functions within complex tissues (Vinken et al., 2006); an electrical synapses in electrically excitable cells (Meier and Dermietzel, 2006, Vinken et al., 2006); a tissue response to hormones (Bian et al., 2015); and a regulatory actors in embryonic development (Oyamada et al., 2013).

A critical role in the progression of a variety of tumours has been attributed to gap junction intercellular communication (Mesnil et al., 2005, Malekian et al., 2016). Most studies show that GJIC is decreased or absent in cancer cells, independently of the origin of the tissue (e.g. glioma, lung, endometrial, breast, cervical or prostate carcinoma), supporting the general assumption that GJIC deficiency is associated with the cancer's phenotype (Mesnil et al., 2005, Leithe et al., 2006). It has been hypothesized that this GJIC reduction in cancer cells, contributes to dysregulated cellular growth by isolating cells from their neighbors (Aftab et al., 2015). Despite the vast majority of neoplastic cells have reduced GJIC compared to their non-neoplastic counterparts (Mesnil et al., 2005, Leithe et al., 2006), there are exceptions in

that some cancer cells have normal or greater gap junction expression and cell-cell coupling (Kapoor et al., 2004, Naus and Laird, 2010). This does not indicate, however, that such cells communicate normally.

Several methods have been used successfully to understand the physiology of cell-to-cell communications, most of them based on dye transfer such as microinjection, scrape loading, gap-fluorescence recovery after photo-bleaching (gap-FRAP), parachute assay, and local activation of a molecular fluorescent probe (LAMP). Others consist in measuring electrical conductance by dual patch clamp or endogenous compounds transference such as radio-labelled nucleotides or intercellular calcium waves (Abbaci et al., 2007). They are useful for multiple applications, including the study of carcinogenesis, metabolism, embryogenesis, etc., but also present several limitations (i.e. invasive methods that alter cell integrity; restrictions to the possibility of carrying out time-lapse experiments; technically challenging and time-consuming; or limited number of cells analysed). The present manuscript describes a new semi-quantitative methodology using a DEP-based lab-on-a-chip platform for the real-time study of Gap junctional intercellular communication that overcomes some of the limitations presented by the conventional methods. For the setting up of this new methodology, we selected the bone tumour niche which is composed of a very complex cellular network with a large variety of cells (e.g. vascular cells, bone cells, immune cells) communicating by means of soluble mediators (e.g. cytokines, growth factors) and direct intercellular interactions (Krzeszinski and Wan, 2015, Shiozawa et al., 2015, Stains and Civitella, 2016). In the study, we performed interactions of osteosarcoma cells with the main cells accessible to their microenvironment (osteoblasts, osteocytes, osteoclasts and endothelial vascular cells).

MATERIALS AND METHODS

Cell cultures

The human osteosarcoma cell line MNNG/HOS and KHOS were purchased from the American Type Culture Collection (ATCC) and maintained in DMEM supplemented with 10% foetal bovine serum (FBS) and 1% penicillin/streptomycin. Human Vascular Endothelial Cells were acquired from the ATCC and cultured in gelatine-coated plates and ECGM2 supplemented media. The mouse MLOY-4 osteocytic cell line was kindly provided by Dr L. Bonewald (University of Missouri, Kansas City, USA). Cells were cultured on collagen-coated dishes and maintained in a modified essential medium (α-MEM) supplemented with 5% FBS, 5% calf serum (CS), and 1% penicillin and streptomycin. Cells were cultured in a humidified 5% CO_2/air atmosphere at 37°C.

Osteoclast differentiation

$CD14^+$ were obtained from peripheral blood mononuclear cells isolated by centrifugation over Ficoll gradient from the blood of healthy donors (Etablissement Français du Sang, Nantes, agreement referenced NTS 2000-24, Avenant n°10). $CD14^+$ cells were magnetically labelled with CD14 microbeads and positively selected by MACS technology (Miltenyi Biotec, Germany). The purity of the cells was assessed by flow cytometry (Cytomics FC500; Beckman Coulter, France) and was > 95%. The $CD14^+$ were cultured in α-MEM medium (Minimum Essential Medium, Lonza, Belgium) supplemented with 10% FBS and differentiated toward osteoclasts in the presence of 25 ng/mL of human Macrophage Colony Stimulating Factor (and 100 ng/mL of human Receptor Activator of Nuclear Factor KappaB Ligand (hRANKL) for 11 days. Multinucleated cells formed with three nuclei and

more were counted after TRAP staining to verify osteoclast differentiation (Duplomb et al., 2008).

Human mesenchymal cells (hMSCs) and osteoblast differentiation

Bone marrow, harvested by iliac crest aspiration from healthy donors was obtained from the "Etablissement Français du Sang" (Nantes, France) with informed consent and ethical approval. Human mesenchymal stem cells (hMSC) were cultured in DMEM supplemented with 10% of FBS, 2 ng/ml of basic fibroblast growth factor (bFGF), 100 U/ml of penicillin/streptomycin, and 2 mM of L-glutamine (proliferation medium). Adherent cells were frozen at passage 2 after characterisation by flow cytometry ($CD45^-$, $CD34^-$, $CD105^+$, $CD73^+$, and $CD90^+$, purity $\geq$ 99%) prior to further experiments. Two hundred thousand hMSCs were seeded in 24-well plates in proliferation medium and allowed to attach and reach confluence (this represented day 0 for hMSC osteogenic differentiation). After 3 days, the medium was changed without bFGF but supplemented with vitamin D3 (10^{-8} M) and dexamethasone (10^{-7} M). Three days later, ascorbic acid (50 ng/ml) and β-glycerophosphate (10 mM) were added to allow mineralisation, detected by alizarin red-S staining as described previously. Osteoblastic markers were identified at 7 and 21 days by quantitative PCR (Duplomb et al., 2008).

Gene silencing

Knockdown of Cx43 using short hairpin RNA (shRNA) in human KHOS cells was obtained by lentiviral cell transduction. Lentiviral particles production was performed using MISSION® shRNA Plasmid DNA targeting Cx43 [TRCN0000059777 (shCx43.1); TRCN0000059776 (shCx43.2) from Sigma-Aldrich)] following the protocols provided with

the ViraPower Lentiviral Expression System (Invitrogen). Cx43 levels after lentiviral cell transduction was evaluated by RT-qPCR and Western blot.

Gap Junction Intercellular Communication (GJIC) analysis

GJIC was determined by the analysis of intercellular dye transfer. Briefly, cells of interest were detached from the respective plates with accutase, to minimise cell membrane receptors damage, and were divided into "acceptor" and "donor" groups as described in Talbot et al. (2013). Acceptor cells were loaded with a DiI solution (Life Technology, France), a non-transferable membrane dye, and donor cells were dyed with calcein-acetoxymethylester (Calcein-AM, Life Technology, France) for 45 min at room temperature. After the incubation period, the cells were washed in PBS to remove excess dye, and resuspended in culture media. Then, a mixture of cells (10^4 cells from each population) was prepared and loaded into the DEPArray™ cartridge to follow the dye coupling. Some experiments were carried out in the presence of 2 mM ethanol, a conventional inhibitor of GJIC (Chiba et al., 1994, Dillon et al., 2013, Mustonen et al., 2005, Noritake, et al., 2015).

DEPArray™ device

DEPArray™ technology is based on the ability of a non-uniform electric field to exert forces on neutral, polarisable particles, such as cells, which are suspended in a liquid (Tellez-Gabriel et al., 2016). This electrokinetic principle, called dielectrophoresis (DEP), can be used to trap cells in DEP cages by creating an electric field above a subset of electrodes in an array that is in counter phase with the electric field of adjacent electrodes. When a DEP cage is moved by a change in the electric field pattern, the trapped cell moves with it. This DEP technology is combined with high quality image-based selection that allowed us to identify, make interact and recover specific

individual cells of interest from complex, heterogeneous samples (http://www.siliconbiosystems.com)(Figure 1A).

Reverse transcription– quantitative Polymerase Chain Reaction (RT-qPCR)

Total RNA was extracted from cultured cells using NucleoSpin®RNAII (Macherey Nagel, Germany). Total RNA was reversed transcribed using the Maxima H Minus First Strand cDNA Synthesis kit (ThermoFisher, France). For the osteoblasts recovered from the DEPArray™, we used the Cell to Ct kit (Ambion, USA) for RNA extraction and RT-PCR reaction following the manufacturer's instructions. Real-time monitoring of PCR amplification of complementary DNA was performed using DNA primers on a CFX96 real-time PCR detector system (Bio-Rad, France) with SYBR Select master Mix (Life technologies, France). Primer sequences are provided in Supplementary Table 1. Master Mix buffer Target gene expression was normalised to glyceraldehyde 3-phosphate dehydrogenase and β2-microglobuline levels in respective samples as an internal standard, and the comparative cycle threshold (Ct) method was used to calculate relative quantification of target mRNAs. Each assay was performed in triplicate.

Western Blot

Cells were lysed in RIPA buffer (Tris pH8 10 mM, EDTA 1mM, NaCl 150 mM, NP40 1%, SDS 0,1%) containing a cocktail of protease and phosphatase inhibitors (1 mM sodium orthovanadate (Na_2VO_4), 1 mM phenylmethylsulforyl fluoride (PMSF), 10 mM sodium fluoride (NaF), 10 mM N-ethylmaleimide (NEM), 2 μg/ml leupeptin and 1 μg/mlpepstatine) at 4°C and sonicated twice for 30s. 50 μg of total protein were then separated by SDS-polyacrylamide gel electrophoresis and transferred to Immobilon-P membranes (Millipore, Billerica, MA, USA). Membranes were immunoblotted with anti-Connexin43

(mouse monoclonal antibody, dilution 1/1000, Sigma) and or anti-β-actin (rabbit polyclonal antibody, dilution 1/1000, Sigma) antibodies.

Fluorescence quantification

We quantify the transference of calcein from the donor cell to the receptor cell using ImageJ software (v1.49, NIH). We manually drew an outline around the cell/s of interest using circle, polygon free tools, and we measured the following parameters: integrated intensity, area and mean gray value. Also we calculated the intensity of fluorescence for the background, selecting three different areas adjacent to the cell. The total corrected cellular fluorescence (TCCF) = integrated density of selected cell – (area of selected cell × mean fluorescence of background readings), was calculated (Supplementary Figure 1). Each measure was repeated three times independently.

Statistical analysis

Each investigation was reproduced three times in independent experiments. Results were analyzed with the unpaired Mann-Whitney *U* test using two- tailed *p* values. Results are given as mean±SD and results with $p < 0.05$ were considered as significant. Statistical calculations were performed with the SPSS software (version 21.0; SPSS, Chicago, IL, USA).

RESULTS

Setting-up programmable cell-cell interaction and time-lapse imaging

We used different human cell lines to set up a protocol to perform cell-cell interactions in the DEPArray™ and further analysis of GJIC in a time-dependent manner. Two cell populations of interest were labelled with different fluorochroms: DiI and Calcein, red and green fluorescent respectively, mixed at 1:1 ratio and injected into the DEPArray™ cartridge. Individual movements of cells were manually programmed within the chip in predetermined spatial coordinates and afterwards forced cell-cell interaction at different ratios in Calcein-DiI stained cells (Figure 1B). To monitor the transference of Calcein to DiI stained cells and then to evaluate functional GJIC, time lapse imaging for the capture of fluorescence was programmed.

Human osteosarcoma cells communicate by functional gap junctional intercellular communications

We first investigated the intercellular communications established between human osteosarcoma (hOS) cells and programmed cell-cell interactions in the DEPArray™ using different cell ratios. As shown in Figure 2, the Calcein transfer to DiI stained cells was observed from 2 hours after interaction at ratios 1:1 and 1:3 (calcein stained cells: DiI stained cells). In both cases the transfer of fluorescence between hOS cells increased in a time-dependent manner, and at 6 hours the Calcein was almost totally transferred (67% for 1:1 ratio and 71% for 1:3 ratio, $p<0.01$). At 1:2 and 1:4 ratios, similar results were observed (data not shown), demonstrating that hOS are thus able to communicate by means of functional GIJC. A treatment with ethanol abolished the dye transfer between hOS cells, demonstrating the involvement of GJIC in this process (Supplementary Data 2).

Functional gap junctional intercellular communications between osteosarcoma cells and cells that form the bone tumour microenvironment depends on the differentiation state of osteoblastic cells

The bone microenvironment is a very complex system in which many homotypic or heterotypic cell-cell interactions take place. We thus studied the GJIC between human osteosarcoma (hOS) cells and the bone cells present in the bone tumour niche such as osteoblasts, osteoclasts or osteocytes. To elucidate the GJIC between hOS cells and osteoblasts, four independent experiments were performed using osteoblasts at different stages of differentiation: undifferentiated mesenchymal stem cells (MSC), and MSC after 7 and 21 days of differentiation into osteoblasts. As expected, the expression of *RUNX2* and *ALP*, which play critical roles in osteoblast differentiation and osteoblastogenesis respectively, was directly correlated with the stage of MSC differentiation (Figure 3A). Interestingly, establishing functional GJIC between hOS and osteoblasts was dependent on the stage of differentiation of the bone cells (Figure 3B-D). Osteoblast precursors (MSC) were unable to interact with hOS by means of functional GJIC, as revealed by the absence of fluorescence transfer between hOS and this cell line (Figure 3B). Similarly, osteocytes were not able to interact with hOS by means of functional GJIC, as revealed by the absence of fluorescence transfer between hOS and both cell lines (Supplementary Figure 3). On the contrary, Figures 3C and 3D show that hOS cells and osteoblasts at both early and late stages of differentiation (7 and 21 days) interacted together through functional GJIC. We did not observe any difference in these forms of cell communication in relation to the ratio of interacting cells. These observations are correlated with the expression of CX43 which is lower in mesenchymal stem cells than in osteoblasts (Figure 3A).

Osteoclasts and hOS cells do not communicate by Gap junctions

Osteoclasts are the second main cellular component that controls bone metabolism. We initiated cell-cell interactions between pre-osteoclasts (monocytes $CD14^+$) and differentiated $TRAP^+$ osteoclasts [at 5 and 11 days of RANKL treatment (Figure 4 A-C)]. As shown in Figure 4, no transference of Calcein from $CD14^+$ monocytes or from osteoclasts to hOS cells was observed in any of the experimental conditions used, showing that hOS and monocytic lineage do not interact by means of functional GJIC.

Demonstration of functional Gap Junctional Intercellular Communication between human vascular endothelial cells and osteosarcoma cells

The vascular system is essential for both tumour progression and tumour cell extravasation during the metastatic process (Hicklin and Ellis, 2005). In this context, GJIC between human vascular endothelial cells (hVEC) and human osteosarcoma cells was assessed. Calcein transfer was observed from hVEC to hOS cells after 3 hours of cell interaction at different ratios, showing that functional communication had been established between both cell types by means of GJIC (Figure 5).

Inhibition of Gap Junctional Intercellular Communication in knockdown CX43 cells

Cx43 has been described as an essential protein for the formation of Gap junctions (Aftab et al., 2015). In order to determine if the transference of Calcein to DiI stained cells was linked specifically with the GAP junctions, we carried out cell-cell interactions studies by using the DEPArra^{yTM} approach in Cx43 knockdown osteosarcoma cells (Figure 6). Osteosarcoma cells transduced with Cx43-shRNA were characterized by a marked decrease of Cx43 gene expression as shown by RT-qPCR compared to the control shRNA and the parental cell lines (Figure 6A). Western blot analysis revealed that the level of Cx43 protein

simultaneously downregulated confirming the Cx43 knockdown efficacy of the shRNA used (Figure 6B). Interestingly, in contrast to shRNA control transduced cells in which the dye transfer was maintained between osteosarcoma cells (Figure 6C), the calcein transference was totally abolished in Cx43-shRNA modified cells (Figure 6D). The knockdown experiments demonstrated that the calcein transference between osteosarcoma cells were Cx43 dependent and confirmed the results obtained in the presence of a connexin inhibitor (Supplementary Figure 2).

DISCUSSION

It is well-known that Gap Junctional Intercellular Communication is related to cancer (Cronier et al., 2009), but little data is available concerning the role of GJIC in osteosarcoma, specifically with regard to the presence of functional GJIC between tumour cells and the cells that make up the bone tumour microenvironment. To study this physiological process, several methodologies are available, although they have several limitations (Abbaci et al., 2007). In an attempt to better describe the Gap communications established between the different components present in the bone microenvironment, for the first time we used a protocol based on di-electrophoretic forces. The use of DEPArray™ technology for assessing GJIC has several advantages in relation to current techniques in use: i) this technique is not an invasive method and maintains cell integrity; ii) it is possible to recover cells after interaction for further analysis; iii) the number of interacting cells can be controlled easily; iv) it is possible to programme a time lapse to analyse GJIC in real time; v) the system makes it possible to detect up to 5 different fluorochromes, and vi) it is possible to conduct the experiment with a minimal quantity of cells and to analyse dye transfer at the "single cell" level. Despite all the advantages of this methodology, there are nevertheless a certain number of limitations, such as: i) the size of the cells studied, which should be between 7 and 40 µm; ii) the experimental conditions, such as temperature (all the experiments are carried out at 25ºC) or media, are quite restrictive with a potential impact of their viscosity on cell mobility. Indeed, the cell mobility is directly related to the viscosity of their environment and must be between 1 and 1.5 cP; iii) the absence of any extracellular matrix may have an impact on the Gap junction formed (Imbeault et al, 2009).

The DEPArray™ technology allowed us to define a dynamic vision of the GJIC established between the different cell types that make up the bone tumour microenvironment (Figure 7). The inhibition of Calcein transference observed in the presence of a connexin

inhibitor and in Cx43-knockdown osteosarcoma cells confirmed the key role played by the Cx43 in GJIC process (Aftab et al., 2015). Our assessment of functional GJIC in HOS cells done by DEPArray™ microfluidic approach is in agreement with a recent new high throughput screening proposed by Lee et al. (2015) in the cell line. Interestingly, this manuscript did not alter cell viability and we cultured pools of cells and single cells after parachute assay and after recovery step by the DEPArray™ (Data not shown). Similarly, the GJIC between tumour cells and vascular endothelial cells demonstrated in this manuscript was in agreement in the literature. The close contact between invasive cancer cells and endothelial cells is a preliminary step for metastasis. This step is necessary for the extravasation of tumour cells into the bloodstream. A complex process of recognition occurs between the two cell types during this crucial phase (Pollmann et al., 2005, Saito-Katsuragi et al. 2007). In line with several studies (Gramsch et al. 2001, Matemba et al. 2006), we found an increase in Cx43 expression in the differentiated osteoblasts. This may explain why we observed GJIC between hOS cells and differentiated osteoblasts at either 7 or 21 days, whereas no cell-cell communication was observed between osteoblast precursors (MSC) and tumour cells. In addition, it is well-known that the formation of Gap junctions is necessary for the maturation process of osteoblasts (Lloyd and Donahue, 2010). In addition, it has previously been demonstrated that human precursors and mature osteoclasts express Cx43, which appears to be related to osteoclastogenesis (Matemba et al., 2006, Schilling et al., 2008, Stains and Civitella, 2016). One crucial question is now to determine whether or not osteoclasts/osteoblasts are able to communicate together using GJIC. The present data are not in favour of this hypothesis because we did not observe GJIC between human osteoclasts and hOS cells using the DEPArray™ approach. However, the formation of functional GJIC between these two cell types in humans cannot be totally excluded in adherent cell conditions. Future research will be directed towards increasing our knowledge in this area. The

DEPArray™ technology makes it possible to manipulate up to 5 different populations in the same experiment (5 different fluorochromes). This can be used to perform cell-cell interactions with more than two populations, as a means of determining to what extent such multiple interactions have an impact on GJIC functionality. As this technique makes it possible to recover cells after homotypic and heterotypic interactions, the idea is to analyse the mRNA expression of previously determined markers, and to compare expression in non-interacting cells. The use of drugs targeting Gap junctions has important implications in GJIC which can in turn have a direct impact on the progression of cancer. This methodology provides a new means of studying the effect of these drugs with greater accuracy.

ACKNOWLEDGEMENTS

This paper was written as a part of a research project which received funding from the Seventh Framework Programme ([FP7/2007-2013]) under grant agreement n°264817 – BONE-NET. This work was also supported by the Bone Cancer Research Trust (UK, research project number 144681).

AUTHOR CONTRIBUTION AND CONFLICT OF INTEREST STATEMENT

This study was directed and coordinated by DH. MTG, FV and DH designed the experiments. MTG, CC, BBL, MM and HKB carried out the experimental work. All the authors contributed equally to the data analysis and interpretation of the results. MTG, DH and FV prepared the manuscript.

All the authors declare that there is no conflict of interest.

REFERENCES

Abbaci, M., Barberi-Heyob, M., Stines, J. R. , Blondel, W. , Dumas, D., Guillemin, F. Didelon, J., 2007. Gap junctional intercellular communication capacity by gap-FRAP technique: a comparative study. Biotechnol. J. 2, 50-61.

Aftab, Q., Sin, W.C., Naus, C.C., 2015. Reduction in gap junction intercellular communication promotes glioma migration. Oncotarget 6, 11447-11464.

Bian, O., Zhang, H., Guan, Q., Sun, Y., Zeng, D., 2015. High-dose insulin inhibits gap junction intercellular communication in vascular smooth muscle cells. Mol. Med. Rep. 12, 331-336.

Chiba, H., Sawada, N., Oyamada, M., Kojima, T., Iba, K., Ishii, S., Mori, M.,1994. Hormonal regulation of connexin 43 expression and gap junctional communication in human osteoblastic cells. Cell Struct. Funky., 19, 173-177.

Cronier, L., Crespin, S., Strale, P.O., Defamie, N., Mesnil, M. 2009. Gap junctions and cancer: new functions for an old story. Antioxid. Redox Signal 11, 323-338.

Dillon, J., Andrianakis, I., Mould, R., Ient, B., Liu, W., James, C., O'Connor, V,, Holden-Dye, L., 2013. Distinct molecular targets including SLO-1 and gap junctions are engaged across a continuum of ethanol concentrations in Caenorhabditis elegans. FASEB J. 27, 4266-4278.

Duplomb, L., Baud'huin, M., Charrier, C., Berreur, M., Trichet, V., Blanchard, F., Heymann, D., 2008. Interleukin-6 inhibits receptor activator of nuclear factor kappaB ligand-induced osteoclastogenesis by diverting cells into the macrophage lineage: key role of Serine727 phosphorylation of signal transducer and activator of transcription 3. Endocrinology 149, 3688-3697.

Firestone, G.L., Kapadia, B.J., 2012. Minireview: regulation of gap junction dynamics by nuclear hormone receptors and their ligands. Mol. Endocrinol. 26, 1798-1807.

Tellez-Gabriel, M., Rodiguez-Calleja, L.R., Chalopin, A., Ory, B., Heymann, D., 2016.

Circulating Tumor Cells: A Review of Non-EpCAM-Based Approaches for Cell Enrichment and Isolation. Clin. Chem. 62, 571-581.

Gramsch, B., Gabriel, H.D., Wiemann, M., Grummer, R., Winterhager, E., Bingmann, D., Schirrmacher, K., 2001. "Enhancement of connexin 43 expression increases proliferation and differentiation of an osteoblast-like cell line." Exp. Cell Res. 264, 397-407.

Hicklin, D.J., Ellis, L.M. 2005. Role of the vascular endothelial growth factor pathway in tumor growth and angiogenesis. J. Clin. Oncol. 23, 1011-1027.

Imbeault, S., Gauvin, L.G., Toeg, H.D., Pettit, A., Sorbara, C.D., Migahed, L., DesRoches, R., Menzies, A.S., Nishii, K., Paul, D.L., Simon, A.M., Bennett, S.A., 2009. The extracellular matrix controls gap junction protein expression and function in postnatal hippocampal neural progenitor cells. B.M.C. Neurosci. 10, 13.

Kapoor, P., Saunders, M.M., Li, Z., Zhou, Z., Sheaffer, N., Kunze, E.L., Samant, R.S., Welch, D.R., Donahue, H.J., 2004. Breast cancer metastatic potential: correlation with increased heterotypic gap junctional intercellular communication between breast cancer cells and osteoblastic cells. Int. J. Cancer 111, 693-697.

Krzeszinski, J.Y., Wan, Y., 2015. New therapeutic targets for cancer bone metastasis. Trends Pharmacol. Sci. 36, 360-373.

Lee, J.Y., Choi, E.J., Lee J., 2015. A new high-throughput screening-compatible gap junctional intercellular communication assay. B.M.C. Biotechnol. 15, 90.

Leithe, E., Sirnes, S., Omori, Y., Rivedal, E., 2006. Downregulation of gap junctions in cancer cells. Crit. Rev. Oncog. 12, 225-256.

Lloyd, S.A., Donahue, H.J., 2010. Gap Junctions and Biophysical Regulation of Bone Cells. Clin. Rev. Bone Miner. Metab. 8, 189-200.

Malekian, N., Habibi, J., Zangooei, M.H., Aghakhani, H., 2016. Integrating evolutionary game theory into an agent-based model of ductal carcinoma in situ: Role of gap junctions in cancer progression. Comput. Methods Programs Biomed. 136, 107-117.

Matemba, S.F., Lie, A., Ransjo, M., 2006. Regulation of osteoclastogenesis by gap junction communication. J. Cell Biochem. 99, 528-537.

Meier, C., Dermietzel, R., 2006. Electrical synapses-gap junctions in the brain. Results Probl. Cell Differ. 43, 99-128.

Mesnil, M., Crespin, S., Avanzo, J.L., Zaidan-Dagli, M.L., 2005. Defective gap junctional intercellular communication in the carcinogenic process. Biochim. Biophys. Acta 1719, 125-145.

Mustonen, H., Kiviluoto, T., Paimela, H., Puolakkainen, P., Kivilaakso, E., 2005. Calcium signaling is involved in ethanol-induced volume decrease and gap junction closure in cultured rat gastric mucosal cells.Dig. Dis. Sci. 50, 103-110.

Naus, C.C., Laird, D.W., 2010. Implications and challenges of connexin connections to cancer. Nat. Rev. Cancer 10, 435-441.

Nielsen, M.S., Axelsen, L.N., Sorgen, P.L., Verma, V., Delmar, M., Holstein-Rathlou, N.H., 2012. Gap junctions. Compr. Physiol. 2, 1981-2035.

Noritake, K., Aki, T., Funakoshi, T., Unuma, K., Uemura, K., 2015. Direct Exposure to Ethanol Disrupts Junctional Cell-Cell Contact and Hippo-YAP Signaling in HL-1 Murine Atrial Cardiomyocytes. PLoS One **1**0, e0136952.

Oyamada, M., Takebe, K., Endo, A., Hara, S., Oyamada, Y., 2013. Connexin expression and gap-junctional intercellular communication in ES cells and iPS cells. Front Pharmacol. 4, 85.

Pollmann, M.A., Shao, Q., Laird, D.W., Sandig, M., 2005. Connexin 43 mediated gap junctional communication enhances breast tumor cell diapedesis in culture. Breast Cancer Res. 7, R522-534.

Saito-Katsuragi, M., Asada, H., Niizeki, H., Katoh, F., Masuzawa, M., Tsutsumi, M., Kuniyasu, H., Ito, A., Nojima, H., Miyagawa, S., 2007. Role for connexin 26 in metastasis of human malignant melanoma: communication between melanoma and endothelial cells via connexin 26. Cancer 110, 1162-1172.

Schilling, A.F., Filke, S., Lange, T., Gebauer, M., Brink, S., Baranowsky, A., Zustin, J., Amling, M., 2008. Gap junctional communication in human osteoclasts in vitro and in vivo. J. Cell. Mol. Med. 12, 2497-2504.

Shiozawa, Y., Eber, M.R., Berry, J.E., Taichman, R.S., 2015. Bone marrow as a metastatic niche for disseminated tumor cells from solid tumors. Bonekey Rep. 4, 689.

Stains, J.P., Civitella, R., 2106. Connexins in the skeleton. Semin. Cell Dev. Biol. 50, 31-9.

Talbot, J., Brion, R., Picarda, G., Amiaud, J., Chesneau, J., Bougras, G., Stresing, V., Tirode, F., Heymann, D., Redini, F., Verrecchia, F., 2013. Loss of connexin43 expression in Ewing's sarcoma cells favors the development of the primary tumor and the associated bone osteolysis. Biochim. Biophys. Acta 1832, 553-564.

Vinken, M., Vanhaecke, T., Papeleu, P., Snykers, S., Henkens, T., Rogiers, V., 2006. Connexins and their channels in cell growth and cell death. Cell Signal 18, 592-600.

Zhang, S.S., Shaw R.M., 2013. Multilayered regulation of cardiac ion channels. Biochim. Biophys. Acta 1833, 876-885.

FIGURE LEGENDS

Figure 1: Schematic representation of the DEPArray™ experiment to study functional Gap Junctional Intercellular Communication. A) DEPArray™ technology is based on dielectrophoretic forces to trap cells in DEP cages. When a DEP cage is moved by a change in the electric field pattern, the trapped cell moves with it. **B)** Different steps for cell-cell interaction in the DEPArray. Heterogeneous distribution in the cartridge of two different stained cell populations (Calcein and DiI) (1). Program different cell-cell interactions, moving cells to different spatial coordinates (2). Force cells to interact (3). Monitor transference of Calcein to DiI cells by taking different time lapse pictures (4).

Figure 2: Time-lapse imaging of the homotypic Gap Junctional Intercellular Communication between human osteosarcoma cells. Calcein transfer to DiI stained cells was observed from 4 hours after interaction at a ratio of 1:1 and from 2 hours after promoting cell-cell interactions at a ratio of 1:3. The yellow circles indicate the cells on which the intensity of fluorescence was measured. * $p<0.01$.

Figure 3: The establishment of Gap Junctional Intercellular Communication between human osteosarcoma cells and osteoblasts is linked to the cell differentiation stage of the mesenchymal stem cells (MSC). A) Determination of ALP and RUNX mRNA expression by RTqPCR. **(B-D**) Images and calcein tranfer quantification from MSC, osteoblasts at 7 and 21 days of differentiation to hOS cells, respectively. We capture images at 0, 2, 4 and 6 hours after interaction. The yellow circles indicate the cells on which the intensity of fluorescence was measured. * $p<0.05$.

Figure 4: Gap Junctional Intercellular Communication between human osteosarcoma cells and osteoclasts. (A-C) Analysis of calcein transfer from $CD14^+$ monocytes, osteoclasts at 5 and 11 days of RANKL treatment (upper) and the corresponding TRAP image (bottom) analysis. The yellow circles indicate the cells on which the intensity of fluorescence was measured.

Figure 5: Gap Junctional Intercellular Communication between human osteosarcoma cells and vascular endothelial cells. Calcein transference from hVEC to hOS cells was observed from 3 hours at different ratios 1:1 **(A)** and 1:2 **(B).** The yellow circles indicate the cells on which the intensity of fluorescence was measured. * $p<0.01$.

Figure 6: DEPArray™ imaging of dye transfer in Cx43-shRNA knockdown osteosarcoma cells. (A) Cx43 gene expression determined by RT-qPCR, in KHOS parental cell line (P), transduced with two different Cx43-shRNA (shCx43.1 And shCx43.2) and two concentrations of lentiviral particles (a and b) or with a scramble shRNA (shCT). **(B)** Cx43 expression was analysed at the protein level by Western blot. Both Cx43-shRNA used decreased markedly the protein expression of the non-phosphorylated (P0) and phosphorylated forms of Cx43. (**C)** Calcein transfer to DiI stained cells was observed from 3 hours after interaction at a ratio of 1:1 in cells transduced with shControl as observed by the DEPArray™ assay. (**D**) No transfer of Calcein to DiI stained cells was observed in Cx43 knockdown osteosarcoma cells. The yellow circles indicate the cells on which the intensity of fluorescence was measured. ** $p<0.01$.

Figure 7: Gap Junction Intercellular Communications in the bone tumour niche. Communications through Gap junctions were established in a homotypic fashion between

osteosarcoma cells, and in a heterotypic manner between osteosarcoma cells, pre-osteoblasts and differentiated osteoblasts. Osteosarcoma cells did not establish GJIC with either osteoclasts or pre-osteoblasts. Dashed lines indicate the establishment (green) and the absence (red) of GJIC.

Figure 1

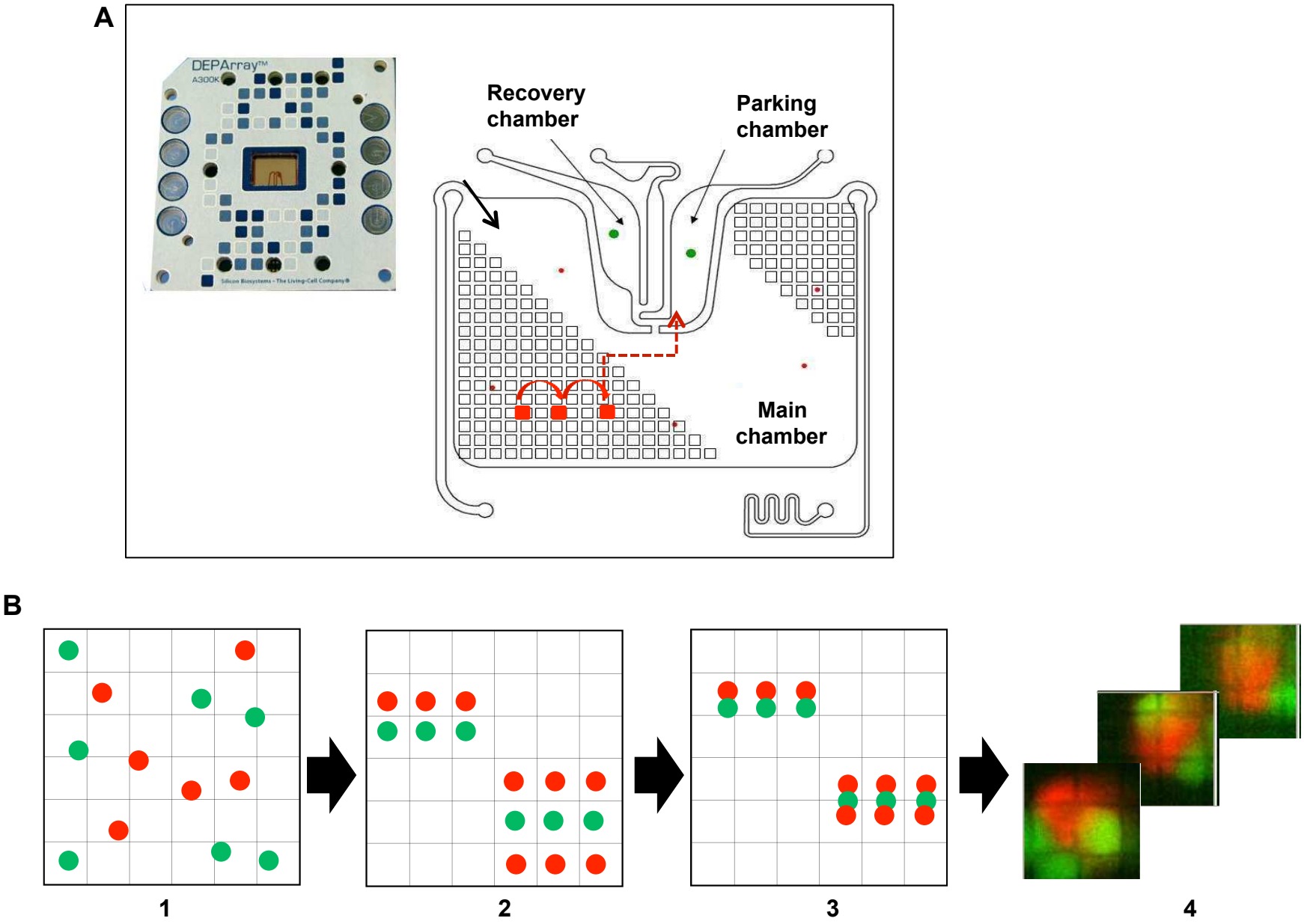
A
DEPArray™
A300K
Recovery chamber
Parking chamber
Main chamber
B
1
2
3
4

Figure 2

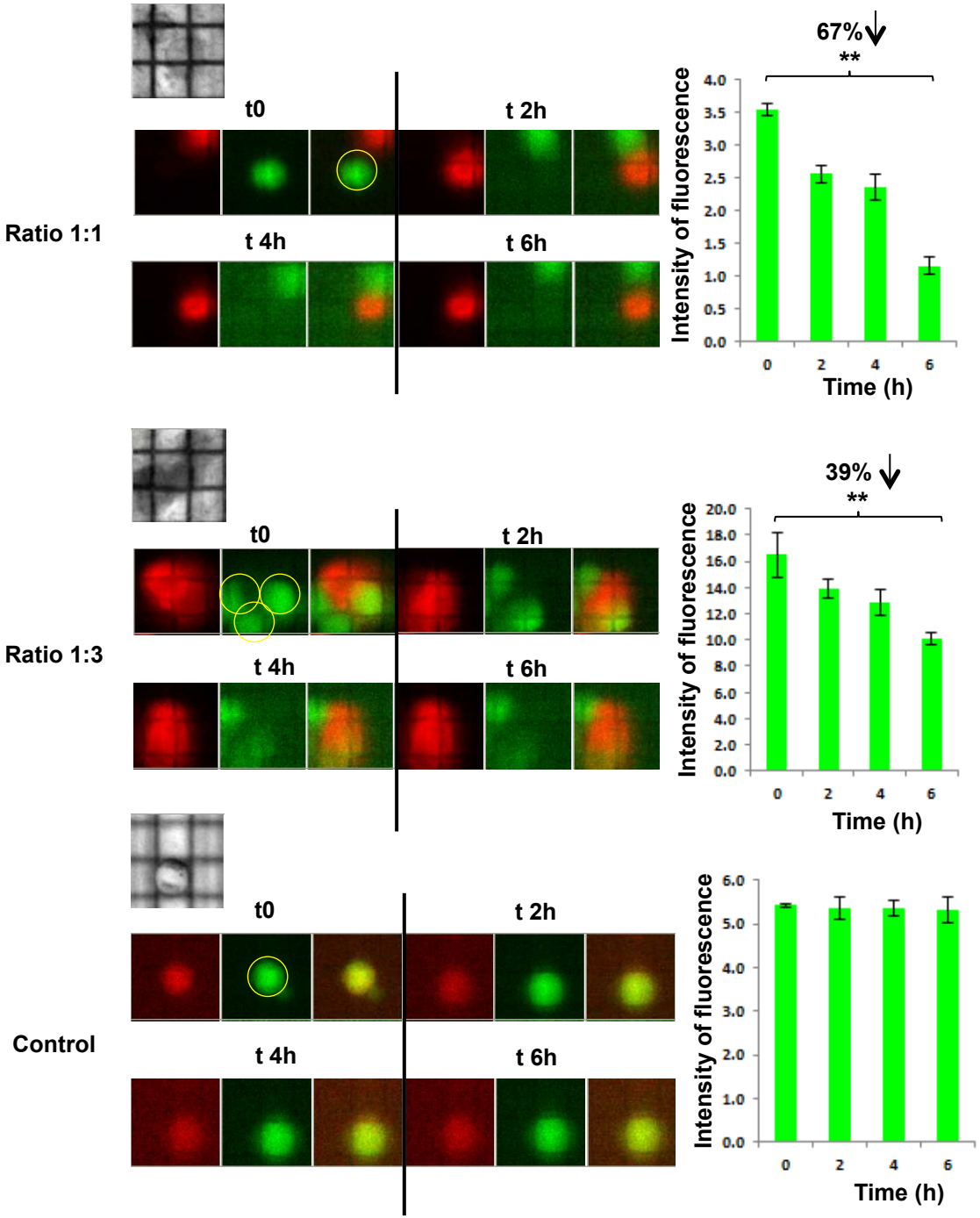
Ratio 1:1
t0
t 2h
t 4h
t 6h
67%
**
Intensity of fluorescence
Time (h)
Ratio 1:3
39%
Control

Figure 3

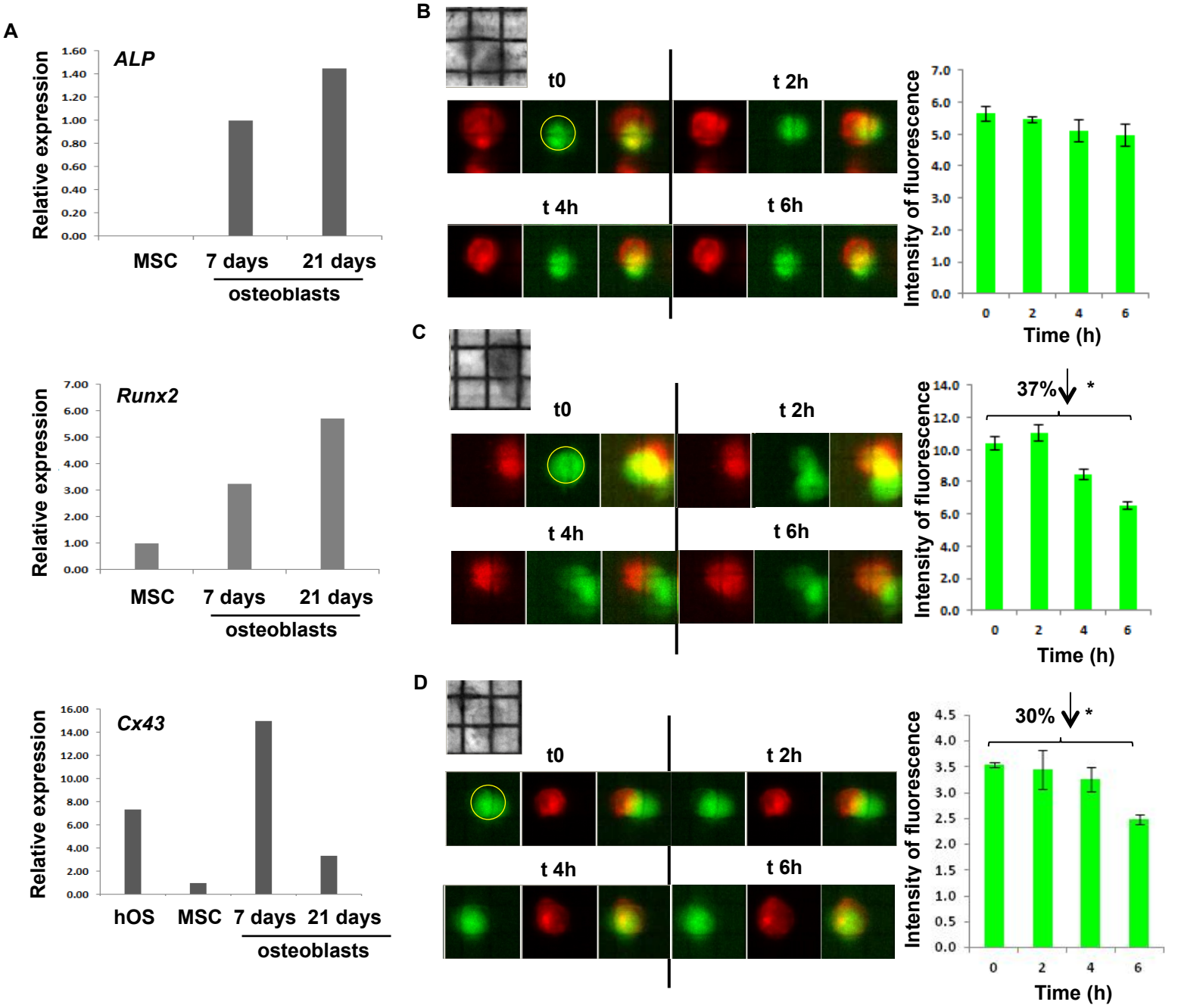
A
ALP
Relative expression
1.60
1.40
1.20
1.00
0.80
0.60
0.40
0.20
0.00
MSC
7 days
21 days
osteoblasts
Runx2
Relative expression
7.00
6.00
5.00
4.00
3.00
2.00
1.00
0.00
MSC
7 days
21 days
osteoblasts
Cx43
Relative expression
16.00
14.00
12.00
10.00
8.00
6.00
4.00
2.00
0.00
hOS
MSC
7 days
21 days
osteoblasts
B
t0
t 2h
t 4h
t 6h
Intensity of fluorescence
7.0
6.0
5.0
4.0
3.0
2.0
1.0
0.0
0
2
4
6
Time (h)
C
t0
t 2h
t 4h
t 6h
37%
*
Intensity of fluorescence
14.0
12.0
10.0
8.0
6.0
4.0
2.0
0.0
0
2
4
6
Time (h)
D
t0
t 2h
t 4h
t 6h
30%
*
Intensity of fluorescence
4.5
4.0
3.5
3.0
2.5
2.0
1.5
1.0
0.5
0.0
0
2
4
6
Time (h)

Figure 4

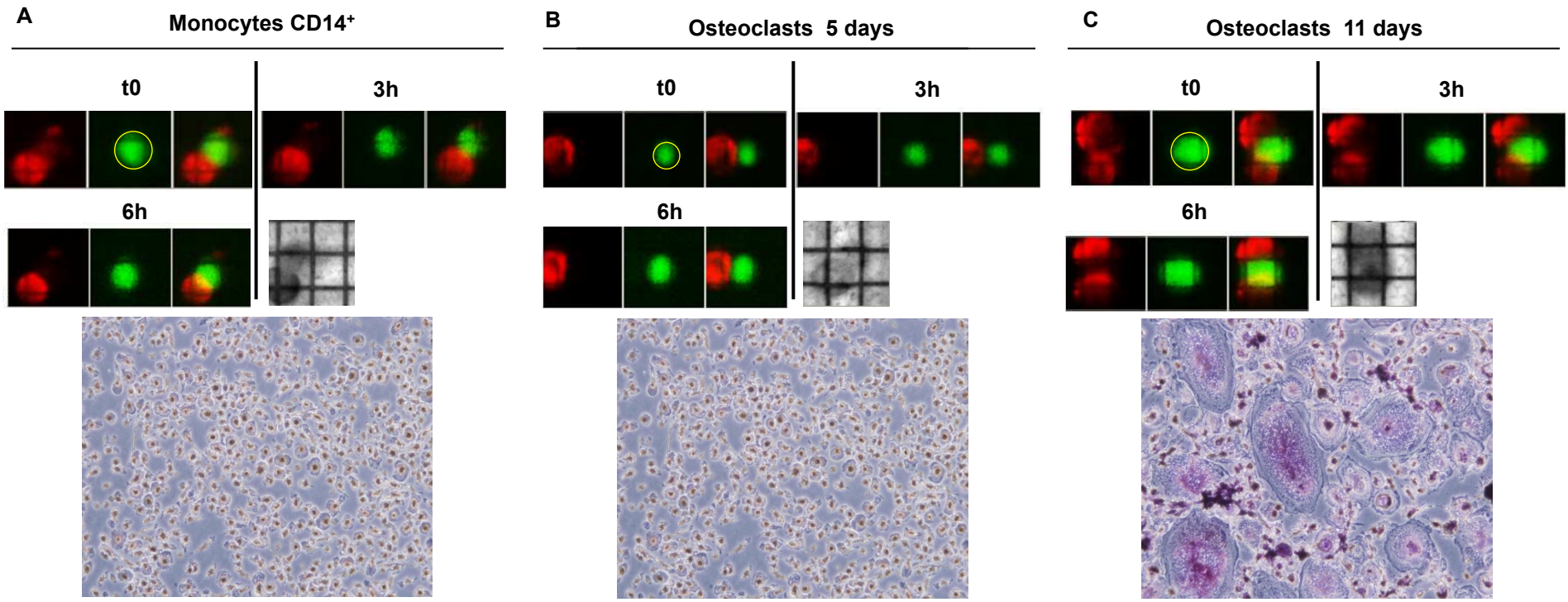
A
Monocytes CD14+
t0
3h
6h
B
Osteoclasts 5 days
t0
3h
6h
C
Osteoclasts 11 days
t0
3h
6h

Figure 5

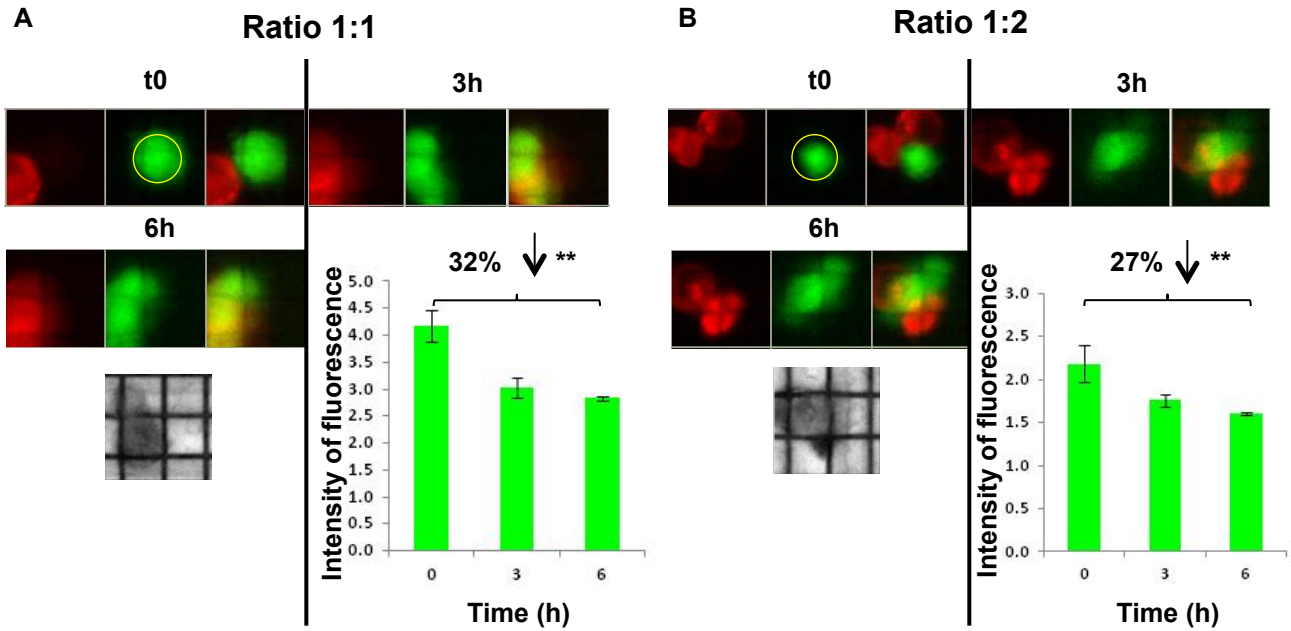
A
Ratio 1:1
t0
3h
6h
32%
**
Intensity of fluorescence
5.0
4.5
4.0
3.5
3.0
2.5
2.0
1.5
1.0
0.5
0.0
0
3
6
Time (h)
B
Ratio 1:2
t0
3h
6h
27%
**
Intensity of fluorescence
3.0
2.5
2.0
1.5
1.0
0.5
0.0
0
3
6
Time (h)

Figure 6

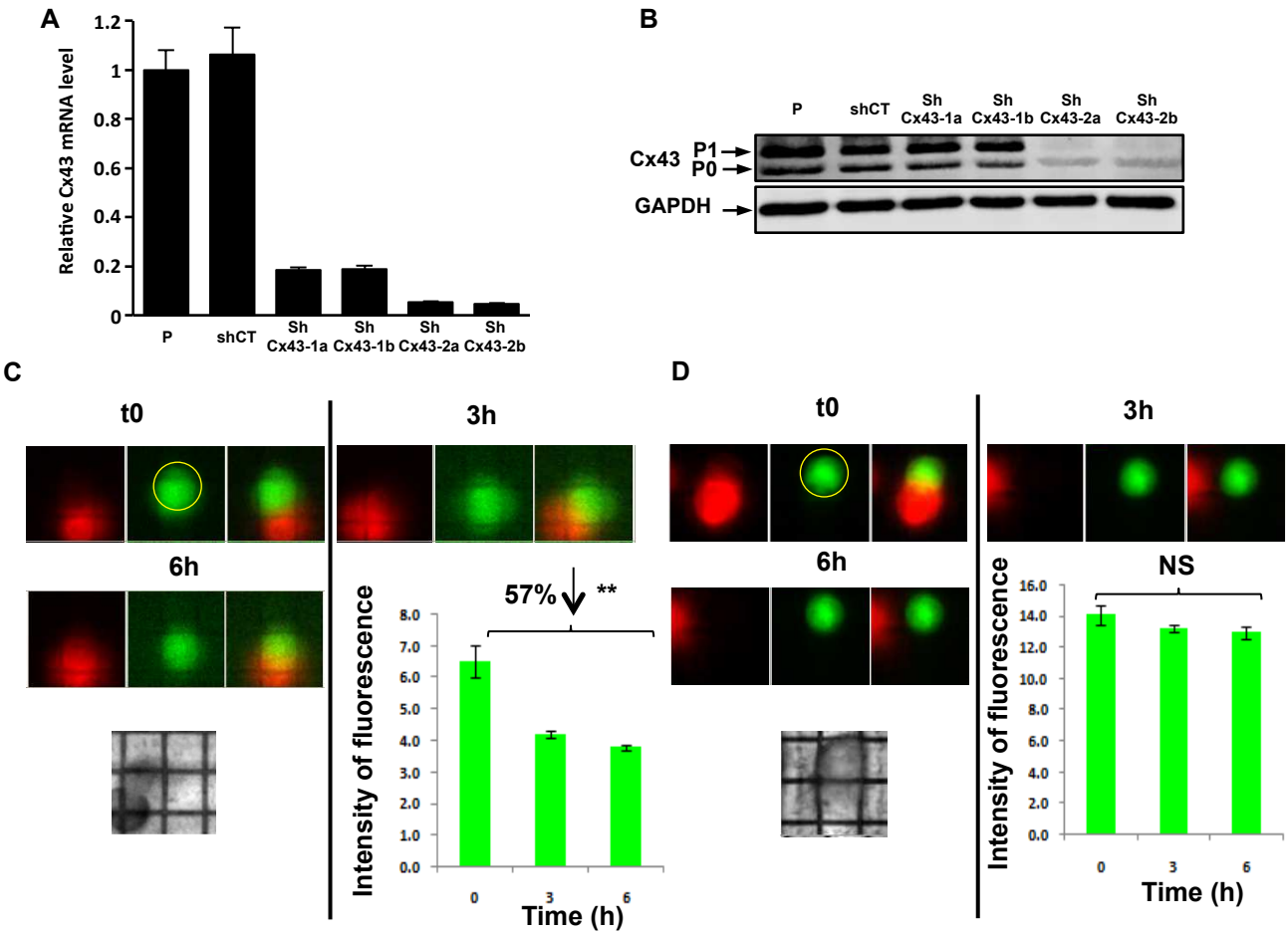
A
Relative Cx43 mRNA level
1.2
1
0.8
0.6
0.4
0.2
0
P
shCT
Sh Cx43-1a
Sh Cx43-1b
Sh Cx43-2a
Sh Cx43-2b
B
P
shCT
Sh Cx43-1a
Sh Cx43-1b
Sh Cx43-2a
Sh Cx43-2b
Cx43
P1
P0
GAPDH
C
t0
3h
6h
57%
**
Intensity of fluorescence
Time (h)
D
t0
3h
6h
NS
Intensity of fluorescence
Time (h)

Figure 7

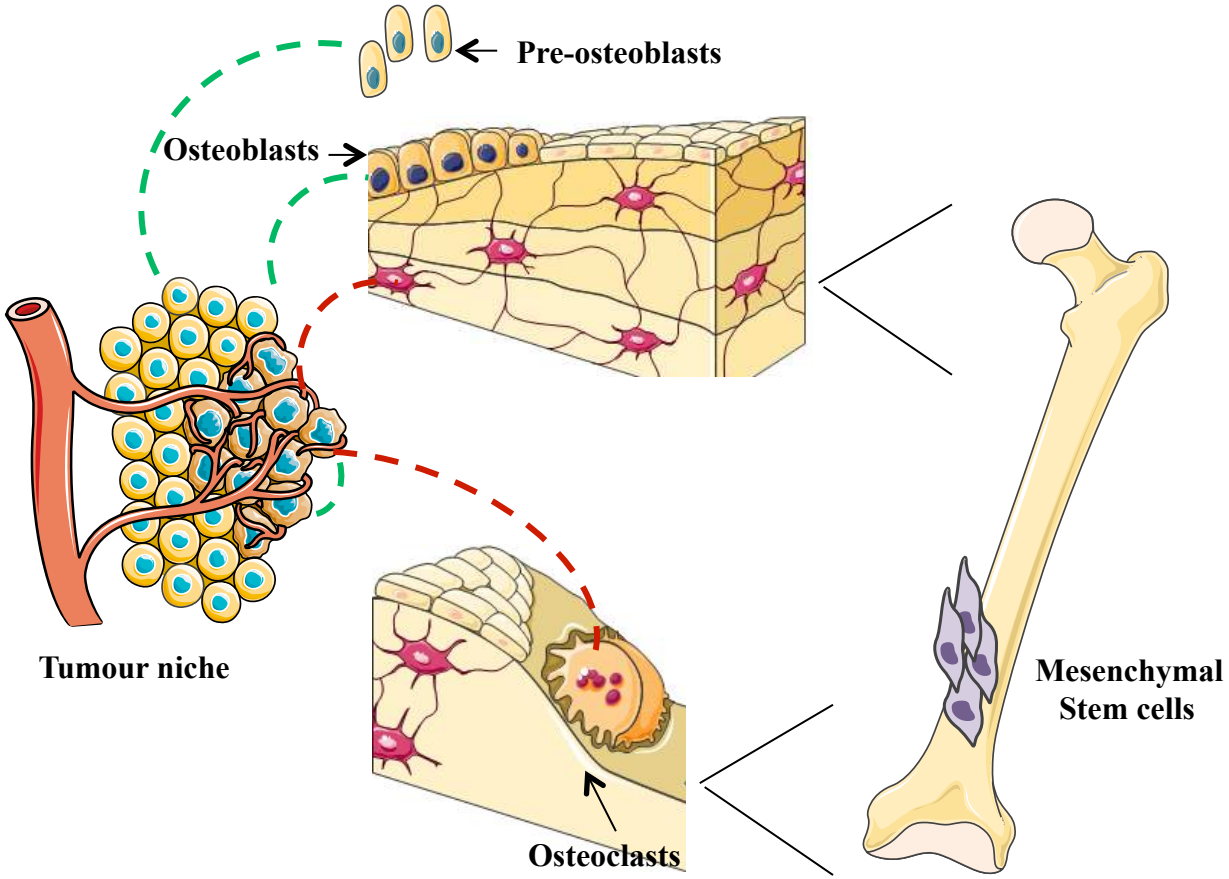
Pre-osteoblasts
Osteoblasts
Tumour niche
Osteoclasts
Mesenchymal
Stem cells

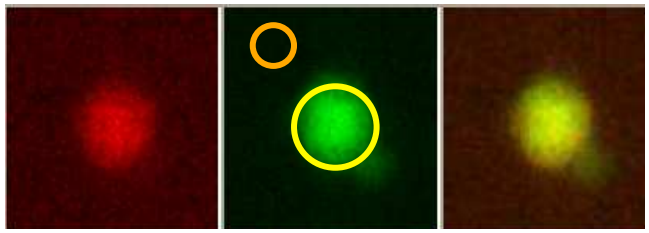

Total corrected cellular fluorescence (TCCF) = integrated density of selected cell – (area of selected cell × mean fluorescence of background readings)

Supplementary Figure 1: Example of the method of fluorescence intensity measurement within cells

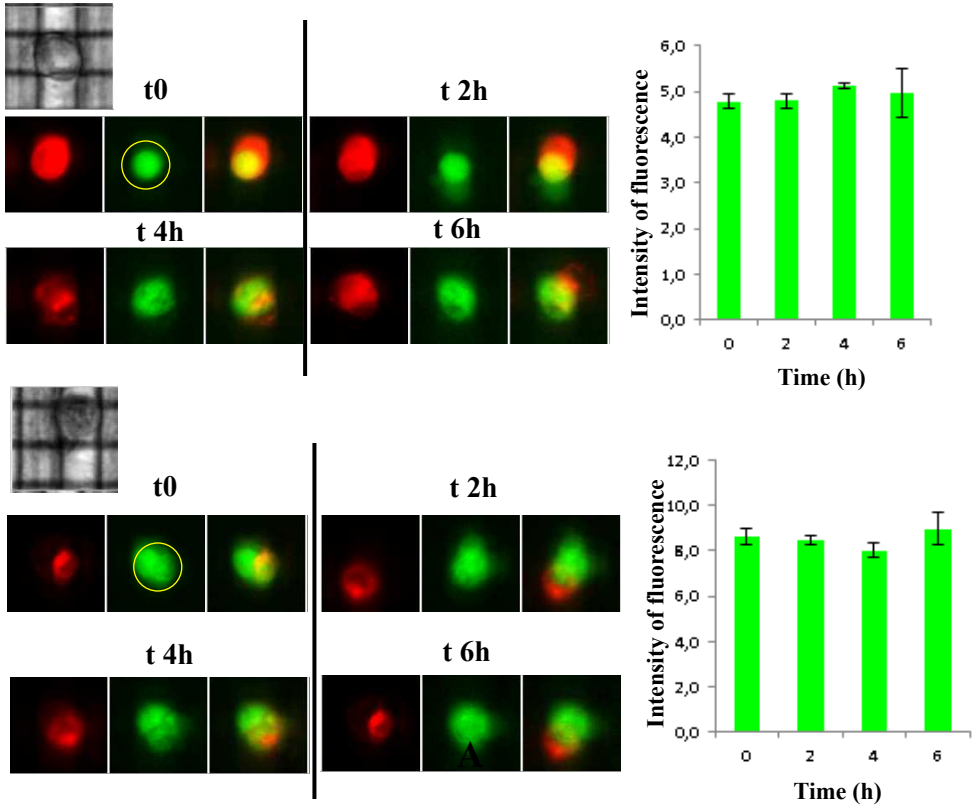

Supplementary Figure 2 : Time-lapse imaging of the homotypic Gap Junctional Intercellular Communication between human MNNG/HOS osteosarcoma cells treated with 2mM ethanol. Cells where treated with ethanol during cell cell interaction time and no transfer of Calcein to DiI stained cells was observed. The yellow circles indicate the cells on which the intensity of fluorescence was measured .

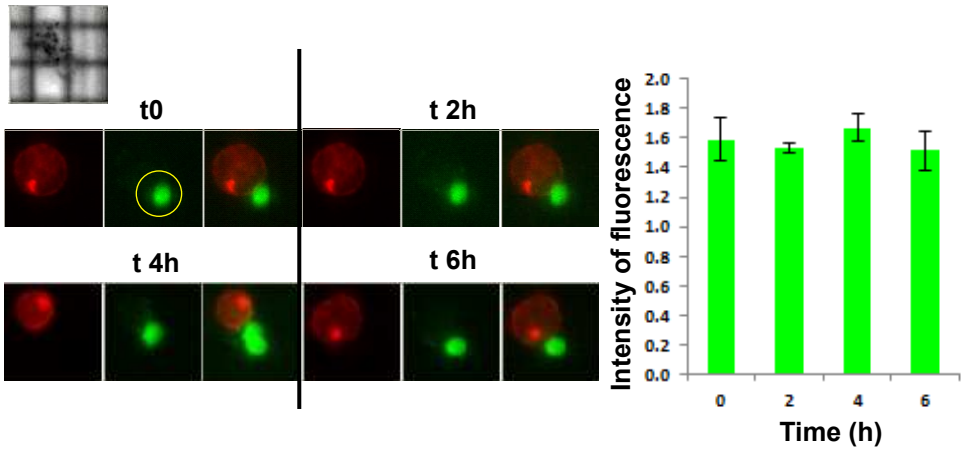

Supplementary Figure 3. Time-lapse imaging of the homotypic Gap Junctional Intercellular Communication between osteocytes and hOS. The transference of Calcein between osteocytes (MLOY-4 cells) and hOS was not observed. The yellow circle indicates the cell on which the intensity of fluorescence was measured in this example. The yellow circles indicates the cells on which the intensity of fluorescence was measured.

Supplementary Table 1: qPCR primers

Gene	Primer Sequences
Human *ALP* (Alkaline Phosphatase)	Fw 5'-AACACCACCCAGGGGAAC-3' Rev 5'-GGTCACAATGCCCACAGATT-3'
Human *Cx43* (Connexin 43)	Fw 5'-GCCTGAACTTGCCTTTTCAT-3' Rev 5'-CTCCAGTCACCCATGTTGC-3'
Human *GAPDH* (Glyceraldehyde 3-phosphate dehydrogenase)	Fw 5'-TGGGTGTGAACCATGAGAAGTATG-3' Rev 5'-GGTGCAGGAGGCATTGCT-3'
Human *RUNX2*	Fw 5'-GCCTAGGCGCATTTCAGA-3' Rev 5'-GCTCTTCTTACTGAGAGTGGAAGG-3'
Human *β2-microglobulin*	Fw 5′- TTCTGGCCTGGAGGCTATC-3′ Rv 5′- TCAGGAAATTTGACTTTCCATTC-3′